Report

Current Biology

Transcriptional Control of Synaptic Remodeling through Regulated Expression of an Immunoglobulin Superfamily Protein

Graphical Abstract

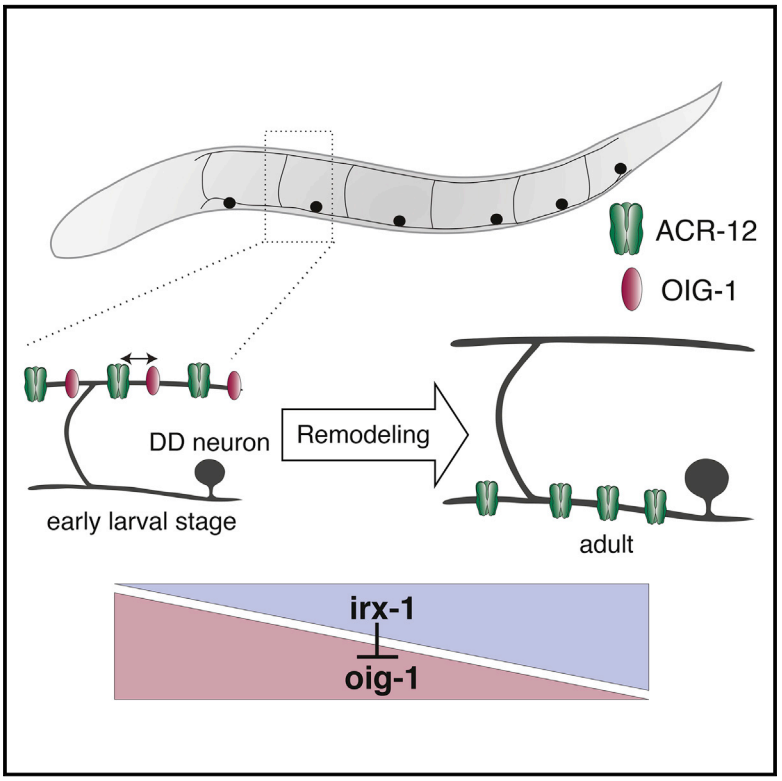

Authors

Siwei He, Alison Philbrook, Rebecca McWhirter, ..., Isabella M. Hanna, Michael M. Francis, David M. Miller III

Correspondence

michael.francis@umassmed.edu (M.M.F.), david.miller@vanderbilt.edu (D.M.M.)

In Brief

Synaptic plasticity is actively regulated in the developing nervous system. He et al. show that the IgSF protein OIG-1 antagonizes the relocation of postsynaptic iACh receptors in *C. elegans* GABAergic neurons. OIG-1 expression is controlled by a transcriptional pathway that orchestrates the synaptic remodeling program.

Highlights

- The IgSF protein OIG-1 antagonizes synaptic remodeling
- OIG-1 blocks the relocation of ACh receptors to new synapses
- IRX-1 downregulates OIG-1 to unleash the remodeling program

Accession Numbers

GSE71618

He et al., 2015, Current Biology *25*, 2541–2548
October 5, 2015
http://dx.doi.org/10.1016/j.cub.2015.08.022

Current Biology
Report

Transcriptional Control of Synaptic Remodeling through Regulated Expression of an Immunoglobulin Superfamily Protein

Siwei He,[1,5] Alison Philbrook,[3,5] Rebecca McWhirter,[2] Christopher V. Gabel,[4] Daniel G. Taub,[4] Maximilian H. Carter,[2] Isabella M. Hanna,[2] Michael M. Francis,[3,*] and David M. Miller III[1,2,*]
[1]Neuroscience Graduate Program, Vanderbilt International Scholar Program
[2]Department of Cell and Developmental Biology
Vanderbilt University, 465 21st Avenue South, Nashville, TN 37240-7935, USA
[3]Department of Neurobiology, University of Massachusetts Medical School, 364 Plantation Street, Worcester, MA 01605, USA
[4]Department of Physiology and Biophysics, Boston University Medical Campus, 700 Albany Street, Boston, MA 02118, USA
[5]Co-first author
*Correspondence: michael.francis@umassmed.edu (M.M.F.), david.miller@vanderbilt.edu (D.M.M.)
http://dx.doi.org/10.1016/j.cub.2015.08.022

SUMMARY

Neural circuits are actively remodeled during brain development, but the molecular mechanisms that trigger circuit refinement are poorly understood. Here, we describe a transcriptional program in *C. elegans* that regulates expression of an Ig domain protein, OIG-1, to control the timing of synaptic remodeling. DD GABAergic neurons reverse polarity during larval development by exchanging the locations of pre- and postsynaptic components. In newly born larvae, DDs receive cholinergic inputs in the dorsal nerve cord. These inputs are switched to the ventral side by the end of the first larval (L1) stage. VD class GABAergic neurons are generated in the late L1 and are postsynaptic to cholinergic neurons in the dorsal nerve cord but do not remodel. We investigated remodeling of the postsynaptic apparatus in DD and VD neurons using targeted expression of the acetylcholine receptor (AChR) subunit, ACR-12::GFP. We determined that OIG-1 antagonizes the relocation of ACR-12 from the dorsal side in L1 DD neurons. During the L1/L2 transition, OIG-1 is downregulated in DD neurons by the transcription factor IRX-1/Iroquois, allowing the repositioning of synaptic inputs to the ventral side. In VD class neurons, which normally do not remodel, the transcription factor UNC-55/COUP-TF turns off IRX-1, thus maintaining high levels of OIG-1 to block the removal of dorsally located ACR-12 receptors. OIG-1 is secreted from GABA neurons, but its anti-plasticity function is cell autonomous and may not require secretion. Our study provides a novel mechanism by which synaptic remodeling is set in motion through regulated expression of an Ig domain protein.

RESULTS AND DISCUSSION

GABAergic DD Motor Neurons Remodel Postsynaptic Components during Larval Development

Motor neurons located in the ventral nerve cord drive locomotion in *C. elegans*. Sinusoidal waves are generated by cholinergic motor neurons that signal at dyadic synapses to excite contraction of ipsilateral body muscles while simultaneously stimulating GABA neurons to induce muscle relaxation on the contralateral side (Figure S1A) [1, 2]. We have previously shown that transgenic expression of a functional ionotropic acetylcholine receptor (iAChR) subunit ACR-12::GFP in GABAergic motor neurons marks these connections with punctate clusters that are closely apposed to cholinergic presynaptic regions labeled with mCherry::RAB-3 (Figures S1B and S1C) [3]. Reconstruction of the DD motor circuit by serial section electron microscopy indicated that cholinergic inputs to DD neurons are switched from dorsal to ventral locations late in the first larval (L1) stage [4]. To confirm this observation, we used the *flp-13* promoter to express both ACR-12::GFP and mCherry::RAB-3 in DD neurons. In this case, ACR-12::GFP clusters are confined to the dorsal side, whereas mCherry::RAB-3-labeled synaptic vesicles are limited to the ventral nerve cord in early L1 larvae (Figures 1A–1C, top). By the adult stage, this configuration is reversed with ACR-12::GFP puncta on the ventral side and mCherry::RAB-3 restricted to presynaptic outputs to dorsal muscles (Figures 1A–1C, bottom). The repositioning of ACR-12::GFP from dorsal to ventral locations was mimicked by another iAChR subunit, UNC-29::GFP, which shows robust expression in GABA neurons (Figures S1D and S1E) [5]. These results confirm that DD remodeling involves a polarity reversal with presynaptic and postsynaptic components switching places at opposite ends of a morphologically intact GABAergic neuron.

In principle, remodeling of the postsynaptic domain could occur either by translocation of existing receptor complexes from the dorsal to the ventral side or by elimination of dorsal receptors and concomitant synthesis of new receptor subunits that assume a ventral position. To distinguish between these possibilities, we used laser microsurgery to sever the commissural process of the DD1 neuron in the early L1 when ACR-12-containing iAChRs

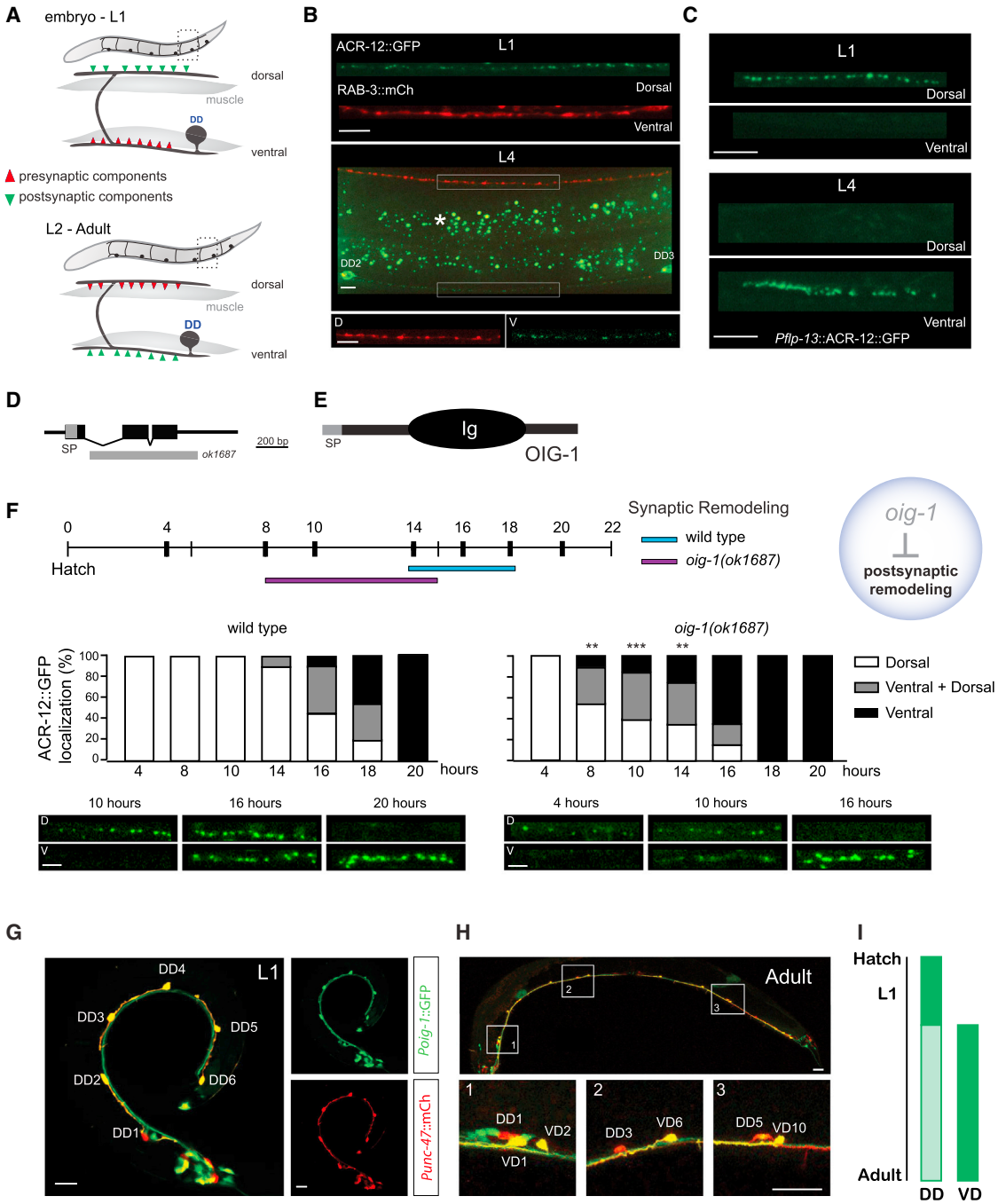

Figure 1. OIG-1 Inhibits Postsynaptic Remodeling of DD Motor Neurons

(A) Embryonic DD motor neurons innervate ventral muscles and extend commissures to the dorsal side for input from cholinergic motor neurons. Toward the end of the L1 larval stage, presynaptic vesicles (red) and postsynaptic acetylcholine receptors (AChRs) (green) switch locations as DDs remodel.

(B) In a newly hatched L1 larva, RAB-3::mCherry (red) marks DD synapses with ventral muscle, and ACR-12::GFP (green) labels postsynaptic DD regions in the dorsal nerve cord. In an L4 larva, presynaptic RAB-3::mCherry (red) labels DD inputs to dorsal muscles and ACR-12::GFP (green) is restricted to ventral DD postsynaptic locations. Asterisk denotes gut autofluorescence. Scale bars, 5 μm.

(C) ACR-12::GFP AChR subunits are dorsally localized in early L1 DD motor neurons but are strictly ventral by the L4 larval stage. Scale bars, 5 μm.

(D) The *oig-1* gene includes three exons (black boxes) with a canonical N-terminal signal peptide (SP) sequence. Exons 2 and 3 are deleted in *oig-1(ok1687)*.

(E) The OIG-1 protein includes an N-terminal signal peptide (SP) and a single immunoglobulin (Ig) domain.

(F) Postsynaptic remodeling is precocious in *oig-1(ok1687)*. Wild-type DD neurons remodel 14–18 hr after hatching, whereas *oig-1* mutant DD neurons remodel 8–16 hr post-hatching. Quantification and representative images of DD remodeling are shown at the bottom. The x axis denotes time since hatching (hr). L1 larvae were binned according to the distribution of *Pflp-13*::ACR-12::GFP puncta as dorsal only (white), ventral only (black), or dorsal and ventral (gray). **p < 0.005, ***p < 0.0005, versus wild-type (dorsal only versus dorsal + ventral and ventral only) (n = 20 for each time point), Fisher's exact test. Scale bars, 2 μm.

(legend continued on next page)

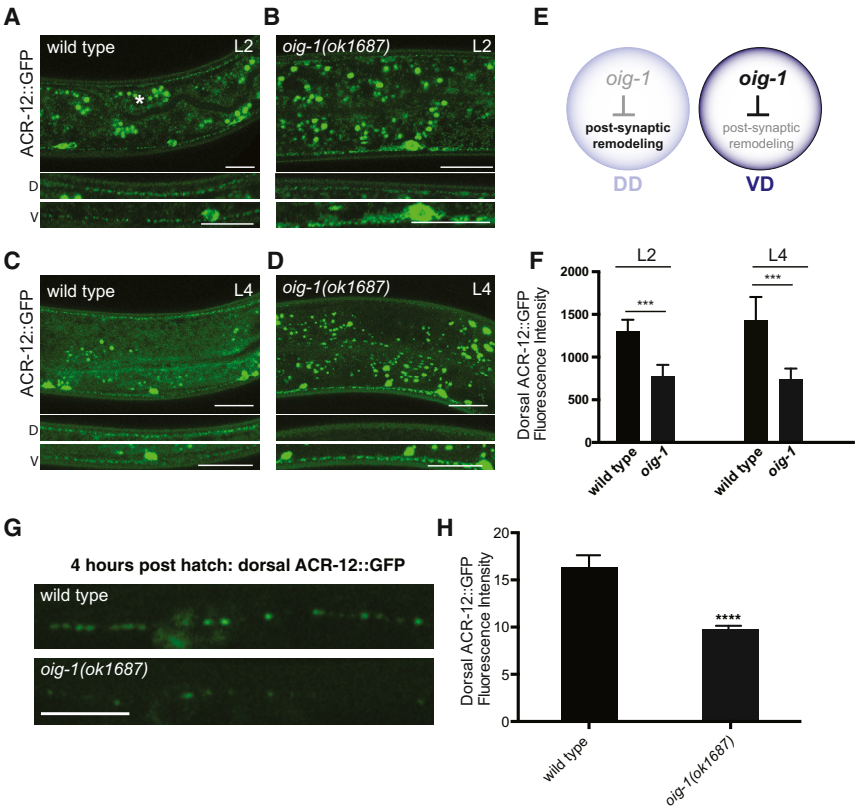

Figure 2. OIG-1 Inhibits Postsynaptic Remodeling of VD Motor Neurons

(A and B) Representative images of *Punc-47*::ACR-12::GFP in L2 wild-type and *oig-1(ok1687)* larvae showing ACR-12::GFP puncta in both dorsal (D) and ventral (V) nerve cords. In *oig-1* mutants, dorsal ACR-12::GFP is significantly reduced compared to wild-type by the L2 stage. Asterisk denotes gut autofluorescence. Scale bars, 20 μm.

(C and D) Representative images of *Punc-47*::ACR-12::GFP puncta in L4 wild-type and *oig-1(ok1687)* larvae. Insets (bottom) show ACR-12::GFP puncta in dorsal (D) and ventral (V) nerve cords. Note depletion of dorsal ACR-12::GFP puncta in *oig-1(ok1687)*. Scale bars, 20 μm.

(E) Model depicting *oig-1* expression in DD and VD motor neurons (L2 – adult) and negative regulation of postsynaptic remodeling.

(F) Quantification of dorsal ACR-12::GFP fluorescence intensity comparing wild-type and *oig-1(ok1687)* L2 and L4 larvae. ***$p < 0.001$, Student's t test, $n > 15$ for each group. Error bars, SD.

(G) Representative images of dorsal ACR-12::GFP puncta in wild-type and *oig-1* mutant L1 animals (4 hr post-hatch). Scale bar, 5 μm.

(H) Quantification of ACR-12::GFP localization in the dorsal nerve cord detects a weaker signal in *oig-1* mutants than in wild-type at 4 hr post-hatch. ****$p < 0.0001$ versus wild-type. $n = 10$ for each group, Student's t test. Error bars, SEM.

are restricted to the dorsal side (Figure S1F). We then monitored the appearance of ACR-12::GFP in the ventral DD1 process and found that ventral ACR-12::GFP clusters were indistinguishable from those in mock-axotomized animals, suggesting that an intact commissural connection between the dorsal and ventral DD processes is not required for postsynaptic remodeling (Figure S1G). These results indicate that ACR-12 receptor translocation from the dorsal to the ventral side is not essential for remodeling and provide evidence that a primary contribution to the ventral receptor pool occurs through de novo ACR-12 synthesis.

An Immunoglobulin Superfamily Protein, OIG-1, Antagonizes Postsynaptic Remodeling of GABAergic Motor Neurons

We used cell-specific microarray analysis to detect strong expression of a transcript encoding a short single-immunoglobulin (Ig) domain protein, OIG-1, in early L1 DD motor neurons (see Supplemental Experimental Procedures) (Table S1) (Figures 1D and 1E). A canonical N-terminal signal peptide predicts that the mature OIG-1 protein (137 amino acids in length) is secreted [6]. Because recent work established that a closely related paralog, OIG-4, stabilizes iAChR complexes in *C. elegans* body muscle cells [7], we wondered whether OIG-1 might exert a similar role and thus potentially retard the dissociation of ACR-12 receptor complexes in remodeling GABA neurons. To address this question, we monitored *Pflp-13*::ACR-12::GFP localization in the null allele, *oig-1(ok1687)* (Figure 1D) and observed that DD postsynaptic remodeling was initiated significantly earlier than in the wild-type (8–16 hr versus 14–18 hr post-hatching) (Figure 1F, top) with the precocious removal of dorsal ACR-12::GFP puncta coinciding with their early appearance on the ventral side (Figure 1F, bottom). This result suggests that OIG-1 normally functions to antagonize the relocation of ACR-12 in L1 stage DD motor neurons (Figure 1F). This model also predicts, however, that OIG-1 expression should be downregulated by the late L1 stage to allow the normal onset of DD remodeling. To test this hypothesis, we used a GFP reporter gene that includes the *oig-1* upstream region (*Poig-1*::GFP) to confirm expression in DD motor neurons in early L1 larvae (Figure 1G) [6, 8]. As development proceeds, the *Poig-1*::GFP signal declines in DD motor neurons but shows strong expression in VD motor neurons beginning soon after their birth at the end of the L1 stage (Figure 1H). This temporal pattern of expression (Figure 1I) prompted us to ask whether OIG-1 is also necessary to prevent the dorsal to ventral translocation of the ACR-12 receptor in VD neurons, which normally do not remodel. Indeed, *oig-1* mutants showed fewer dorsal ACR-12::GFP puncta than wild-type

(G) In L1 larvae, *Poig-1*::GFP is highly expressed in all six DD neurons as shown by co-localization of *Poig-1*::GFP (green) and *Punc-47*::mCherry (red). Scale bars, 10 μm.

(H) By the adult stage, *Poig-1*::GFP is not detected in DD motor neurons but is strongly expressed in VD motor neurons. Insets show representative examples of adjacent DD and VD neurons with differential *Poig-1*::GFP expression. Scale bars, 20 μm.

(I) Schematic denoting periods of strong *Poig-1*::GFP expression (dark green) in developing DD and VD neurons.

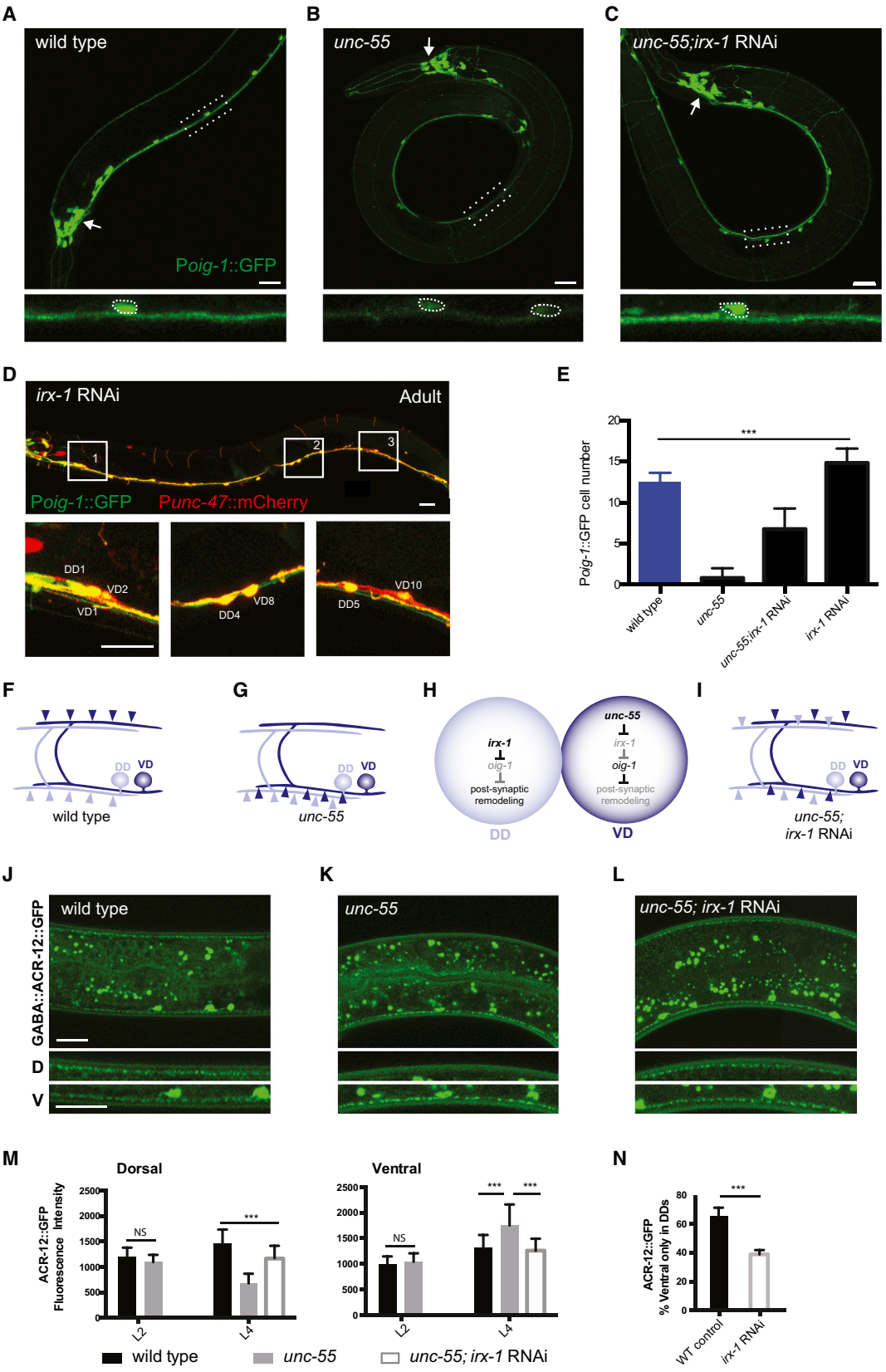

(legend on next page)

in both L2 and L4 larval stages (Figures 2A–2F) and a reciprocal relative increase in ventral ACR-12::GFP (Figure S2G). This result suggests that *oig-1* mutant VD motor neurons undergo ectopic remodeling (e.g., removal of dorsal ACR-12::GFP puncta with reassembly on the ventral side). Notably, *oig-1* mutant animals showed significantly less dorsal ACR-12::GFP than wild-type before remodeling (i.e., 4 hr post hatch), and an overall lower level of ACR-12::GFP in L4 larvae, suggesting that OIG-1 might have an additional role of stabilizing the initial clusters of ACR-12::GFP (Figures 2G and 2H; Figures S2F and S2G).

A Transcriptional Switch Regulates Expression of OIG-1 to Control Postsynaptic Remodeling in GABAergic Neurons

The strong expression of OIG-1 in VD neurons resembles that of the COUP-TF family transcription factor, UNC-55, which has been previously shown to block presynaptic remodeling in VD neurons [9–12]. We thus asked whether OIG-1 is a downstream target of UNC-55. The *Poig-1*::GFP signal is significantly weaker in *unc-55* mutant VD motor neurons but is unaffected in other *Poig-1*::GFP-positive neurons in the head region (Figures 3A, 3B, and 3E). Because UNC-55 is likely to function as a transcriptional repressor [10, 12], we reasoned that this effect should depend on an intermediate target in the *unc-55* pathway. An obvious candidate for this role is the Iroquois family homeodomain transcription factor *irx-1*, which is upregulated in *unc-55* mutant VD motor neurons [12]. Consistent with this model, treatment of *unc-55* mutant animals with *irx-1* RNAi restores *Poig-1*::GFP expression to VD motor neurons (Figures 3C and 3E). *irx-1* RNAi also results in ectopic expression of *Poig-1::*GFP in late larval and adult DD motor neurons (Figures 3D and 3E). These data point to related genetic pathways in which *irx-1* antagonizes *oig-1* expression in DD motor neurons, while *unc-55* blocks *irx-1* expression in VD motor neurons to prevent negative regulation of *oig-1*.

We confirmed the roles of these regulatory cascades in postsynaptic remodeling with additional genetic experiments. In wild-type adults, expression of ACR-12::GFP with the *unc-47* GABA neuron promoter results in comparable levels of postsynaptic ACR-12::GFP clusters on dorsal (VD) and ventral (DD) sides (Figures 3F, 3J, and 3M). At the L2 stage, *unc-55* mutants show a similar distribution of ACR-12::GFP (Figure 3M). Later, in L4 larvae, however, ACR-12::GFP puncta are largely localized to the ventral side of *unc-55* mutants (Figures 3G, 3K, and 3M Figures S2F and S2G). This result suggests that *unc-55* mutant VD neurons initially establish postsynaptic ACR-12 receptor domains in the dorsal nerve cord as in the wild-type, but then reposition these ACR-12::GFP puncta to the ventral side as predicted by our model (Figure 3G). This ectopic postsynaptic remodeling effect in VD neurons can be reversed by global RNAi knockdown of *irx-1* (Figures 3I, 3L, and 3M). Moreover, the ACR-12::GFP remodeling phenotype of *unc-55;oig-1* double mutants is not more severe than that of *oig-1* and shows a slightly weaker phenotype than *unc-55* (Figure S2G). We interpret these findings to indicate that *oig-1* is the principal downstream effector of *unc-55* in a pathway that blocks postsynaptic remodeling in VD neurons. To ask whether *irx-1* is also required for postsynaptic remodeling in DD motor neurons, we used RNAi to downregulate *irx-1* expression in wild-type animals expressing *Pflp-13*::ACR-12::GFP. More than half (66%) of control L1 larvae showed strictly ventral ACR-12::GFP puncta by 27 hr after egg-laying, whereas significantly fewer (39%) of *irx-1* RNAi-treated animals completed postsynaptic remodeling (Figure 3N). The partial remodeling of DD neurons could result from either

Figure 3. A Transcriptional Cascade Involving UNC-55/COUP-TF and IRX-1/Iroquois Regulates *oig-1* Expression in GABA Neurons

All panels depict adults; dorsal is up, and anterior is to left.

(A–C) *Poig-1*::GFP is highly expressed in wild-type VD motor neurons in the ventral nerve cord and in a subset of head neurons (arrow). In *unc-55* mutants, *Poig-1*::GFP is decreased in VD neurons but is maintained in head neurons (arrow). *irx-1* RNAi restores *Poig-1*::GFP expression to ventral cord motor neurons. Insets (bottom) feature enlarged and straightened segments of the ventral nerve cord. Dotted circles denote *Poig-1*::GFP-expressing ventral cord neurons. Scale bars, 20 μm for (A)–(C).

(D) RNAi knockdown of *irx-1* restores *Poig-1*::GFP expression to DD neurons in wild-type adults; *Poig-1*::GFP is maintained in the VDs. Inserts (1, 2, 3) show adjacent DD and VD neurons expressing *Poig-1*::GFP. *Punc-47*::mCherry marks GABAergic motor neurons and was merged with *Poig-1*::GFP images to produce yellow overlays. Scale bars, 20 μm.

(E) Quantification of *Poig-1*::GFP expression in adult ventral cord GABAergic motor neurons. *Poig-1*::GFP is expressed in all 13 VD motor neurons in the wild-type but is rarely detected in the ventral cord of *unc-55* mutants. *Poig-1*::GFP expression is partially restored in *irx-1* RNAi-treated *unc-55* mutants and is ectopically expressed in adult DD neurons with *irx-1* RNAi of wild-type animals. ***$p < 0.001$. One-way ANOVA followed by Tukey multiple comparison test, $n > 30$ for each group. Error bars, SD.

(F and G) In wild-type adults, DD postsynaptic AChRs (light blue) are located on the ventral side, whereas VD postsynaptic receptors (dark blue) are located dorsally. In *unc-55* mutants, postsynaptic ACh receptors are ectopically relocated to the ventral side in VD motor neurons.

(H) Model: IRX-1 is expressed in DD motor neurons to promote postsynaptic remodeling by inhibiting OIG-1 expression. IRX-1 is repressed by UNC-55 in VD motor neurons to prevent ectopic remodeling of postsynaptic components to the ventral side.

(I) *irx-1* RNAi suppresses postsynaptic remodeling of both DD neurons and ectopically remodeled VD neurons in *unc-55* mutants.

(J–L) GABA::ACR-12::GFP (or *Punc-47*::ACR-12::GFP) puncta are detected in both dorsal and ventral nerve cords of wild-type L4 larval animals due to contributions of VD (dorsal) and DD (ventral) neurons (J). In *unc-55* mutants, GABA::ACR-12::GFP puncta are largely ventral (K) but are relocated to the dorsal side in animals treated with *irx-1* RNAi (L). Scale bars, 20 μm for (J)–(L).

(M) Quantification of dorsal and ventral GABA::ACR-12::GFP fluorescence intensity for wild-type (black), *unc-55* (gray), and *unc-55;irx-1* RNAi (white) at L2 and L4 stages. In L2 larvae, the distribution of ACR-12::GFP puncta in the dorsal nerve cord does not differ between *unc-55* versus wild-type indicating that the initial assembly of the VD postsynaptic apparatus is not perturbed in *unc-55* animals. In contrast, in L4 larvae, *unc-55* mutant animals show significantly fewer dorsal ACR-12::GFP puncta than wild-type; this ectopic remodeling effect was blocked by *irx-1* RNAi. ***$p < 0.001$, one-way ANOVA, $n > 15$ for each group. Error bars, SD.

(N) *irx-1* RNAi knockdown delays DD postsynaptic remodeling. By 27 hr after egg laying (16 hr post-hatch), 66% ± 6% of wild-type (WT) control larvae have completed DD remodeling (i.e., show ventral GABA::ACR-12::GFP only), whereas only 39% ± 3% of *irx-1* knockdown animals have completed DD remodeling, ***$p < 0.001$ ($n = 113$), Fisher's exact test. Error bars, SD.

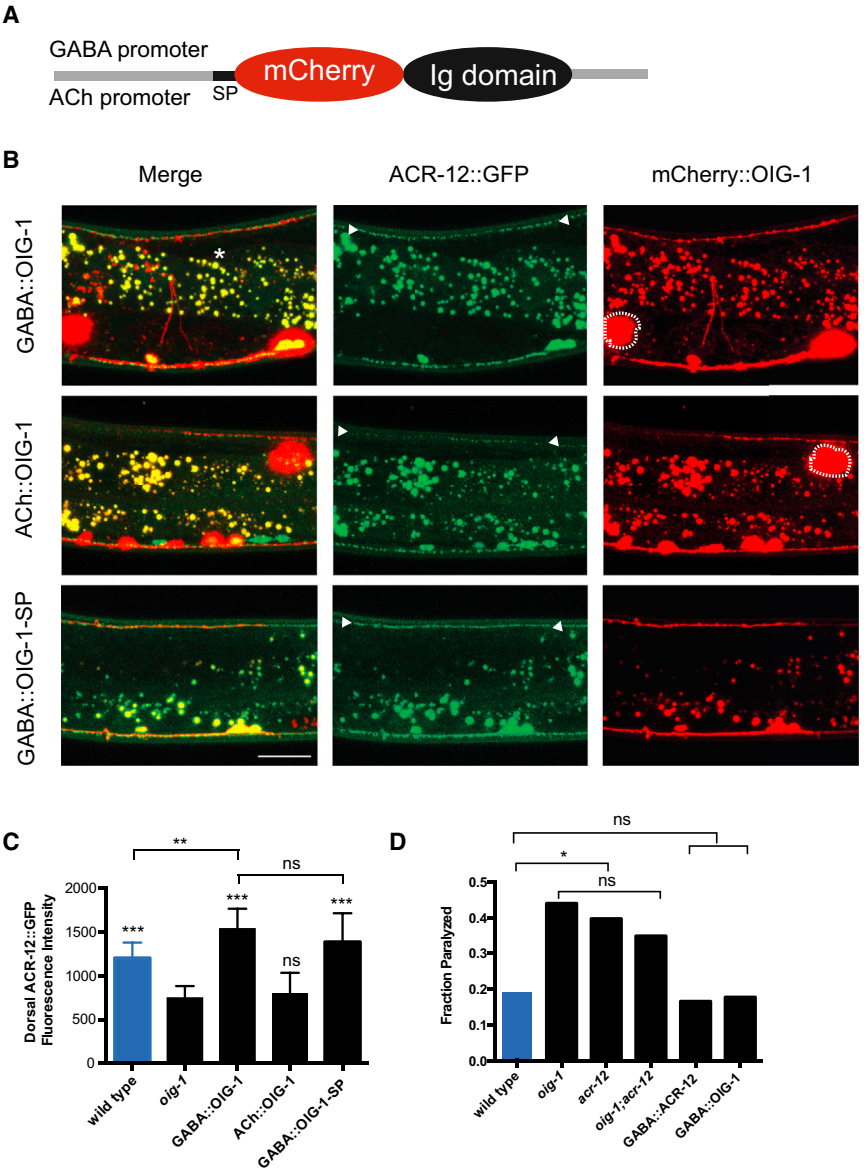

Figure 4. Cell-Autonomous Expression of OIG-1 Blocks Postsynaptic Remodeling in GABA Neurons

(A) Schematic of OIG-1 fusion protein. mCherry was inserted immediately after the OIG-1 signal peptide (SP) and fused to upstream promoters for expression in either GABA or ACh (cholinergic) motor neurons in the ventral nerve cord.

(B) All panels show young adults; anterior is to left, and dorsal is up. Expression of mCherry::OIG-1 in GABA neurons with the *unc-25* promoter (GABA::OIG-1) restores dorsal ACR-12::GFP puncta (arrowheads) to an *oig-1* mutant. mCherry::OIG-1 is detected in both the ventral and dorsal nerve cords and is secreted as indicated by mCherry-labeled coelomocytes (dotted outline) in the body cavity. mCherry::OIG-1 expression in cholinergic motor neurons with the *acr-2* promoter (ACh::OIG-1) does not result in significant restoration of ACR-12::GFP puncta to the dorsal nerve cord (arrowheads), although mCherry-labeled coelomocytes (dotted outline) are indicative of secretion. GABA neuron expression of a non-secreted version of mCherry::OIG-1 (GABA::OIG-1-SP) restores dorsal ACR-12::GFP (arrowheads), suggesting that secretion of the OIG-1 protein may not be required for its function in GABA neuron remodeling. Asterisk denotes gut autofluorescence. Scale bar, 20 μm.

(C) Quantification of dorsal ACR-12::GFP fluorescence intensity in young adults. *oig-1* mutants (black) show reduced dorsal ACR-12::GFP signal versus wild-type (blue). Expression of mCherry::OIG-1 in GABA neurons but not in cholinergic motor neurons restores dorsal ACR-12::GFP to wild-type levels. GABA neuron expression of OIG-1-SP, the non-secreted form of mCherry::OIG-1, also rescues *oig-1*. ***$p < 0.0001$ versus *oig-1*, **$p < 0.001$ versus wild-type, ns ($p > 0.33$), one-way ANOVA followed by Tukey multiple comparison test, $n > 15$ for each experimental group. Error bars, SD.

(D) *acr-12(ok367)* and *oig-1(ok1687)* mutants show locomotory defects that depend on GABA motor neuron function. The number of immobilized L4 larvae at the end of a 10-min swimming assay was determined by direct observation. *oig-1(ok1687)* and *acr-12(ok367)* mutants showed a higher fraction of immobilized animals than wild-type. The swimming defect of *acr-12(ok367)* and *oig-1(ok1687)* can be rescued by expression of ACR-12 (GABA::ACR-12) and OIG-1 (GABA::OIG-1) specifically in GABA neurons, respectively. *$p < 0.05$ versus wild-type. ns, $p > 0.05$, $n > 60$ for each experimental group. All comparisons by Fisher's exact test.

inefficient RNAi knockdown of *irx-1* or the parallel function of another transcriptionally regulated pathway in the DD remodeling program [13]. In any case, the delay in DD remodeling in *irx-1*-RNAi-treated animals requires *oig-1* activity (Figure S2E). Finally, we confirmed that *irx-1* function is cell autonomous in DD and VD neurons using cell-specific RNAi (Figures S2A–S2D). Taken together, our results demonstrate that postsynaptic remodeling in GABA neurons is modulated by the opposing roles of UNC-55 and IRX-1 in the regulation of OIG-1 expression (Figures 3H and S2H). These findings parallel earlier results showing that UNC-55 and IRX-1 also control presynaptic GABA neuron plasticity [12, 13] and thus suggest that this genetic pathway orchestrates the overall remodeling program (see below).

OIG-1 Functions in GABA Neurons to Block Postsynaptic Remodeling

Although OIG-1 is strongly expressed in DD and VD neurons, the OIG-1 protein is predicted to be secreted, and thus could potentially function as an extracellular antagonist of postsynaptic remodeling in a non-autonomous fashion. To test for this possibility, we used transgenic reporters in which mCherry was inserted immediately after the signal peptide (SP) to label the OIG-1 protein (Figure 4A). Expression of the mCherry::OIG-1 construct with the GABA-neuron specific *unc-25* promoter (GABA::OIG-1) resulted in bright punctate mCherry signals along both ventral and dorsal nerve cords (Figure 4B, top). Similar results were obtained using the native promoter driving OIG-1 fused to superfolder GFP (Figures S3A and

S3B). A robust mCherry signal in coelomocytes, macrophage-like cells in the body cavity, confirms that mCherry::OIG-1 is secreted (Figure 4B, top). mCherry::OIG-1 expression in the GABAergic neurons of *oig-1* mutant animals restored dorsal *Punc-47*::ACR-12::GFP to a wild-type level, thus demonstrating that the mCherry::OIG-1 fusion protein is functional and that expression of OIG-1 in GABA neurons is sufficient to rescue the Oig-1 postsynaptic remodeling defect (Figures 4B, top, and 4C). Secretion of mCherry::OIG-1 from neighboring cholinergic neurons (ACh::OIG-1), however, did not rescue the Oig-1 phenotype (Figures 4B, middle, and 4C). This result indicates either that OIG-1 function is cell autonomous and requires expression in GABA neurons or that the secreted form of OIG-1 is not actively involved in postsynaptic remodeling.

To distinguish between these possibilities, we generated a mCherry::OIG-1 protein that excludes the N-terminal signal peptide, thus preventing secretion, and expressed it in GABA neurons [GABA::OIG-1-SP] (see Supplemental Experimental Procedures). Transgenic *oig-1(ok1687)* animals expressing GABA::OIG-1-SP showed strong mCherry puncta in GABA neuron processes in both the dorsal and ventral nerve cords (Figure 4B, bottom). As predicted for a non-secreted form of OIG-1, coelomocytes were not labeled with mCherry in this strain; however, ACR-12::GFP was restored to the dorsal nerve cord indicating strong rescue of the Oig-1 postsynaptic remodeling defect (Figures 4B, bottom, and 4C). We note that transgenic expression of OIG-1 and OIG-1-SP appears to elevate ACR-12::GFP levels in comparison to wild-type perhaps due to the overall role of OIG-1 in stabilizing ACR-12::GFP clusters (Figure 4C). We used a live animal antibody labeling method [14] to further investigate OIG-1 secretion in each situation. The external cell membranes of GABA neurons showed strong immunostaining in animals expressing full-length OIG-1, but no extracellular signal was detected in animals expressing OIG-1-SP (Figure S3C). While we cannot exclude the possibility OIG-1-SP may reach the extracellular environment at low levels that are below the threshold of detection in our experiments, our evidence points to an alternative model in which postsynaptic remodeling does not require the secreted form of OIG-1, but instead involves an intracellular OIG-1 function in GABA neurons. In an additional experiment to define a location for OIG-1 function, we used mosaic expression of a low-copy-number GABA::mCherry::OIG-1 transgene to show that localization of mCherry::OIG-1 puncta to the dorsal nerve cord is correlated with the restoration of dorsal ACR-12::GFP puncta in an *oig-1* mutant (Figures S3E and S3F). This result points to a local role for OIG-1 in antagonizing the removal of ACR-12 receptors by the remodeling program. We note, however, that mCherry::OIG-1 and ACR-12::GFP do not overlap in the dorsal nerve cord but instead adopt a striking pattern of alternating mCherry and GFP puncta (Figure S3G). This finding argues against the idea that OIG-1 stabilizes ACR-12-containing iACh receptors by direct interaction at the synapse and favors an alternative model potentially involving additional components (Figure S4F). The proposed role for OIG-1 in postsynaptic remodeling is further reinforced by our findings that *oig-1* and *acr-12* mutants display similar locomotory defects that depend on GABA neuron dysfunction (Figure 4D).

OIG-1 Inhibits Presynaptic Remodeling in GABAergic Motor Neurons

Having shown that OIG-1 antagonizes postsynaptic remodeling, we next asked whether OIG-1 also regulates the location of presynaptic proteins in the remodeling program. In the wild-type, the presynaptic marker SNB-1::GFP switches from the ventral to the dorsal side in remodeling DD motor neurons, while VD motor neurons synapse with ventral muscles throughout life. These patterns of expression produce a mature GABAergic motor circuit with SNB-1::GFP puncta in both the dorsal (DD) and ventral (VD) nerve cords (Figure S4A). In *unc-55* mutants, however, VD motor neurons undergo ectopic remodeling resulting in the net depletion of ventral SNB-1::GFP puncta (Figures S4C and S4D) [9, 12, 15]. Ventral SNB-1::GFP puncta in the GABAergic circuit are also reduced in *oig-1(ok1687)* versus the wild-type (Figure S4B), suggesting that presynaptic components are ectopically remodeled in *oig-1* mutant VD motor neurons. Our data are consistent with the observation that DD motor neurons show precocious presynaptic remodeling in *oig-1* mutant L1 larvae and that this effect is rescued by cell autonomous OIG-1 function [16]. It is notable, however, that *oig-1* mutants retain a greater number of ventral SNB-1::GFP puncta than observed in *unc-55*, which suggests that ectopic presynaptic remodeling in *oig-1* mutants is incomplete and substantially less severe (Figure S4D). This difference indicates that UNC-55 likely controls an additional parallel-acting pathway involving *irx-1* that regulates presynaptic remodeling (Figure S4E) [12].

Although synaptic refinement is crucial to the creation of a mature nervous system, it may be equally important to maintain the architecture of established circuits by tightly controlling the activation of remodeling pathways. Our results show that the opposing roles of the conserved transcription factors IRX-1/Iroquois and UNC-55/COUP-TF orchestrate both the timing and location of synaptic remodeling in the *C. elegans* GABA motor neuron circuit (Figure S2H). *irx-1* antagonizes *oig-1* expression in late L1 stage DD neurons to permit the disassembly of the postsynaptic apparatus by the remodeling program. This inhibition of *oig-1* is blocked in the VDs by *unc-55*, which turns off *irx-1* and thus maintains high levels of OIG-1 to preserve dorsal clusters of iAChRs (Figure S2H). This negative regulatory pathway appears to function in concert with the PITX homeodomain transcription factor UNC-30, which promotes *oig-1* expression [16] (Figure S4F). However, the role of *unc-30* is likely complex because it is also required for DD expression of *irx-1* [12].

Immunoglobulin superfamily (IgSF) proteins perform central roles in fundamental aspects of neuronal development, including cell migration, growth cone guidance, and synapse formation and function. IgSF proteins may act as cell adhesion molecules (CAMs), secreted ligands or auxiliary subunits that facilitate the function of specific receptors [6, 17–20]. In the case of OIG-1, our work suggests that OIG-1 protein inhibits the disassembly of the ACR-12 receptor complex in a mechanism that opposes remodeling of the postsynaptic region. Given our finding that a non-secreted form of OIG-1 (OIG-1-SP) is functional (Figures 4B and 4C), we suggest that OIG-1 might exert this effect before entering the secretory pathway [21] such that OIG-1-SP could potentially interact with its normal physiological targets. Our results have established a key role for OIG-1 in a mechanism that regulates the relocation of a postsynaptic iAChR from the dorsal

to ventral arms of remodeling GABAergic neurons. We also detected a relatively minor function for OIG-1 in the redistribution of a presynaptic component in the opposite direction (Figures S4A–S4D). The origin of this effect is unclear but could indicate that the removal of the postsynaptic apparatus facilitates assembly of presynaptic components in the same location. By comparison, *unc-55* exerts a strong negative effect on the ectopic relocation of SNB-1 in VD neurons [12], perhaps indicating that other effectors regulated by *unc-55* serve parallel roles in presynaptic remodeling (Figure S4E). We have shown that the IgSF protein OIG-1 antagonizes developmental remodeling of postsynaptic iAChRs in the processes of GABAergic neurons. The molecular mechanism underlying this effect and the components of the remodeling program that OIG-1 opposes are important subjects for future studies.

ACCESSION NUMBERS

The accession number for the microarray data reported in this paper is GEO: GSE71618.

SUPPLEMENTAL INFORMATION

Supplemental Information includes Supplemental Experimental Procedures, four figures, and one table and can be found with this article online at http://dx.doi.org/10.1016/j.cub.2015.08.022.

AUTHOR CONTRIBUTIONS

S.H. generated transgenic lines, collected confocal images, and quantified results for *oig-1*, *irx-1*, and *unc-55* mutant phenotypes. A.P. generated transgenic lines, collected confocal images, and quantified results for *oig-1* mutant effects. R.M. collected and analyzed DD microarray data. A.P., C.V.G., and D.G.T. conducted laser ablation experiments. M.H.C., I.M.H., and S.H. performed the swimming assays. M.M.F. and D.M.M. designed and interpreted experiments and wrote the final document.

ACKNOWLEDGMENTS

We thank members of D.M.M.'s lab and V. Budnik for critical reading of the manuscript and helpful discussions, K. Howell, J. White, and O. Hobert for sharing information before publication, C. Lambert for technical assistance, Y. Jin for strain *juls223*, and E. Lundquist for *Pstr-1::*GFP. Some nematode strains used in this work were provided by the *Caenorhabditis* Genetics Center, which is funded by the NIH National Center for Research Resources (NCRR). This work was supported by NIH grants to D.M.M. (R01NS081259), C.V.G. (R01NS077929), and M.M.F. (R01NS064263). S.H. is partially supported by the Vanderbilt International Scholar Program. A.P. is supported by an NIH predoctoral NRSA (F31DA038399). Experiments were performed in the VMC Flow Cytometry Shared Resource and by VANTAGE (supported by NIH grants, P30 CA68485, DK058404, P30 EY08126, and G20 RR030956).

Received: March 31, 2015
Revised: July 4, 2015
Accepted: August 10, 2015
Published: September 17, 2015

REFERENCES

1. White, J.G., Southgate, E., Thomson, J.N., and Brenner, S. (1986). The structure of the nervous system of the nematode Caenorhabditis elegans. Philos. Trans. R. Soc. Lond. B Biol. Sci. *314*, 1–340.
2. Zhen, M., and Samuel, A.D. (2015). C. elegans locomotion: small circuits, complex functions. Curr. Opin. Neurobiol. *33*, 117–126.
3. Petrash, H.A., Philbrook, A., Haburcak, M., Barbagallo, B., and Francis, M.M. (2013). ACR-12 ionotropic acetylcholine receptor complexes regulate inhibitory motor neuron activity in Caenorhabditis elegans. J. Neurosci. *33*, 5524–5532.
4. White, J.G., Albertson, D.G., and Anness, M.A. (1978). Connectivity changes in a class of motoneurone during the development of a nematode. Nature *271*, 764–766.
5. Spencer, W.C., Zeller, G., Watson, J.D., Henz, S.R., Watkins, K.L., McWhirter, R.D., Petersen, S., Sreedharan, V.T., Widmer, C., Jo, J., et al. (2011). A spatial and temporal map of C. elegans gene expression. Genome Res. *21*, 325–341.
6. Aurelio, O., Hall, D.H., Hobert, O., and Hobert, O. (2002). Immunoglobulin-domain proteins required for maintenance of ventral nerve cord organization. Science *295*, 686–690.
7. Rapti, G., Richmond, J., and Bessereau, J.L. (2011). A single immunoglobulin-domain protein required for clustering acetylcholine receptors in C. elegans. EMBO J. *30*, 706–718.
8. Cinar, H., Keles, S., and Jin, Y. (2005). Expression profiling of GABAergic motor neurons in Caenorhabditis elegans. Curr. Biol. *15*, 340–346.
9. Walthall, W.W., and Plunkett, J.A. (1995). Genetic transformation of the synaptic pattern of a motoneuron class in Caenorhabditis elegans. J. Neurosci. *15*, 1035–1043.
10. Shan, G., Kim, K., Li, C., and Walthall, W.W. (2005). Convergent genetic programs regulate similarities and differences between related motor neuron classes in Caenorhabditis elegans. Dev. Biol. *280*, 494–503.
11. Zhou, H.M., and Walthall, W.W. (1998). UNC-55, an orphan nuclear hormone receptor, orchestrates synaptic specificity among two classes of motor neurons in Caenorhabditis elegans. J. Neurosci. *18*, 10438–10444.
12. Petersen, S.C., Watson, J.D., Richmond, J.E., Sarov, M., Walthall, W.W., and Miller, D.M., 3rd. (2011). A transcriptional program promotes remodeling of GABAergic synapses in Caenorhabditis elegans. J. Neurosci. *31*, 15362–15375.
13. Thompson-Peer, K.L., Bai, J., Hu, Z., and Kaplan, J.M. (2012). HBL-1 patterns synaptic remodeling in C. elegans. Neuron *73*, 453–465.
14. Gottschalk, A., and Schafer, W.R. (2006). Visualization of integral and peripheral cell surface proteins in live Caenorhabditis elegans. J. Neurosci. Methods *154*, 68–79.
15. Hallam, S.J., and Jin, Y. (1998). lin-14 regulates the timing of synaptic remodelling in Caenorhabditis elegans. Nature *395*, 78–82.
16. Howell, K., White, J.G., and Hobert, O. (2015). Spatiotemporal control of a novel synaptic organizer molecule. Nature *523*, 83–87.
17. Rougon, G., and Hobert, O. (2003). New insights into the diversity and function of neuronal immunoglobulin superfamily molecules. Annu. Rev. Neurosci. *26*, 207–238.
18. Ding, M., Chao, D., Wang, G., and Shen, K. (2007). Spatial regulation of an E3 ubiquitin ligase directs selective synapse elimination. Science *317*, 947–951.
19. Woo, J., Kwon, S.-K., Nam, J., Choi, S., Takahashi, H., Krueger, D., Park, J., Lee, Y., Bae, J.Y., Lee, D., et al. (2013). The adhesion protein IgSF9b is coupled to neuroligin 2 via S-SCAM to promote inhibitory synapse development. J. Cell Biol. *201*, 929–944.
20. Kolodkin, A.L., and Tessier-Lavigne, M. (2011). Mechanisms and molecules of neuronal wiring: a primer. Cold Spring Harb. Perspect. Biol. *3*, a001727–a001727.
21. Ast, T., Cohen, G., and Schuldiner, M. (2013). A network of cytosolic factors targets SRP-independent proteins to the endoplasmic reticulum. Cell *152*, 1134–1145.

